International Journal of Thermophysics, Vol. 17, No. 5, 1996

High-Temperature, High-Pressure Thermophysical Measurements on Liquid Zinc[1]

C. Otter,[2] G. Pottlacher,[2,3] and H. Jäger[2]

Wire-shaped zinc samples were resistively volume heated as part of a fast-capacitor discharge circuit. Time-resolved measurements with submicrosecond resolution of the current through the specimen, the voltage drop across it, and the thermal expansion of the specimen as a function of time allow determination of the enthalpy, electrical resistivity, and density at different temperatures up to superheated liquid states of zinc far above the normal boiling point. High static pressures, up to 3800 bar of the ambient medium water, were used. An estimate of the critical pressure for zinc is given by investigations of the stability of the sample with a framing CCD camera, taking pictures of different samples varying the ambient static pressure. The critical volume and the critical temperature are obtained by means of an extrapolation of measured data at different pressures.

KEY WORDS: critical point; electrical resistivity; enthalpy; high pressure; high temperature; liquid metals; zinc.

1. INTRODUCTION

During recent years, there has been an increasing demand for thermophysical data on liquid metals and alloy. Properties of matter at high temperatures are useful for high-temperature technologies such as in aerospace and nuclear energy, for modeling of casting processes by numerical simulation, and to obtain phase diagrams.

There is only a limited amount of data for critical-point parameters of metals available, and for most metals they can be deduced only from theoretical models. A limited number of metals have critical pressures lower

[1] Paper presented at the Fourth International Workshop on Subsecond Thermophysics, June 27–29, 1995, Köln, Germany.

[2] Institut für Experimentalphysik, Technische Universität Graz, Petersgasse 16, A-8010 Graz, Austria.

[3] To whom correspondence should be addressed.

0195-928X/96/0900-0987$09.50/0

than 4000 bar, such as lead [1] and indium [2]. A summary of theoretical estimations selected by Ohse and Tippelskirch [3] gave indications that the critical pressure for zinc is also lower than 4000 bar. Therefore, we have continued our work on critical-point data by studying zinc in the liquid phase. The results obtained allow an estimation of the critical-point parameters of zinc from pressure-dependent measurements.

2. MEASUREMENTS

A fast pulse-heating technique was used to investigate liquid zinc. The samples were resistively heated from room temperature far into a superheated liquid state by passing a large current pulse trough them from a capacitor bank. Wire-shaped zinc samples of 99.99+ purity (Goodfellow Metals, Cambridge, UK) were used, with a typical length of 40 mm and a diameter of 0.5 mm. From time-resolved measurements of current, voltage, and thermal expansion, the temperature dependence of the following thermophysical properties were obtained: enthalpy, density, and electrical resistivity for the liquid phase.

Experiments were conducted in a pressure vessel under different ambient static pressures from atmospheric pressure up to 3800 bar to have nearly isobaric conditions. The ambient pressurizing medium was water.

The main emphasis of this work was investigation of the strong volume expansion of the sample at different pressures (called "phase explosion"; see Fig. 1), in the vicinity of the spinodal line in the phase diagram. For static pressures above the critical pressure, the phase explosion should vanish, as discussed later in detail. Therefore, the sample radius is monitored with a fast-framing CCD camera, which takes pictures of the diameter of a small part of the sample every 9 μs.

This camera (Fa. PCO, Computer Optics, Germany) uses a charge-coupled device sensor, with an array of 576×384 pixels. A gatable multichannel plate in front of the chip operates as an amplifier and shutter. The chip itself is masked with a metal foil, which covers most of the sensitive area of the chip. Only at the top margin of the chip does a window of 32×384 pixels remain open. These 32 pixel rows are exposed and then shifted into the dark, covered zone, with a minimum time of 9 μs. Determined by the geometry of the chip, 18 exposures, with a time shift of 9 μs between each frame, can be taken. When the chip is full, the stored information is read by a personal computer with the help of an image converting system in a slow scan mode (SIS, Fa. Theta Systems, Germany). Figure 1 shows a picture with nine frames in a row. Starting with the top frame, which is triggered at a prechosen instant, the second frame shows the same spot of the sample, after a time shift of 10.13 μs, as always used for the zinc

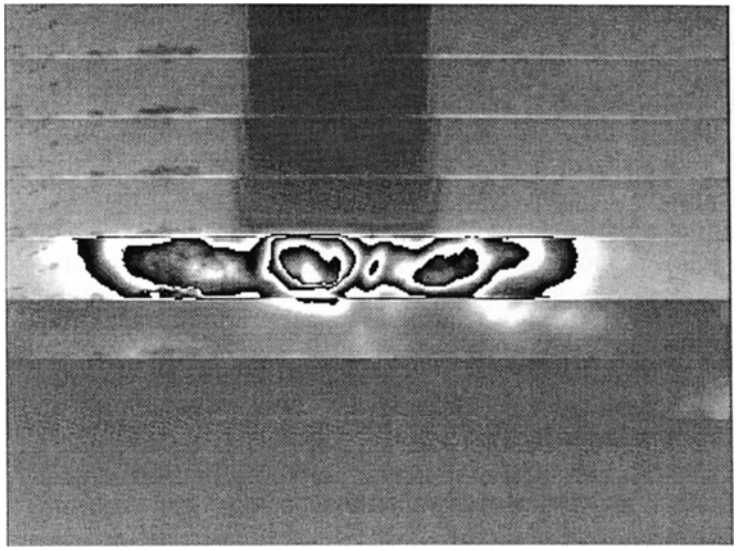

Fig. 1. Phase explosion of a zinc samplers picture taken with a fast-framing CCD camera. The phase explosion can be seen in the fifth frame from the top, 45.5 μs after the start of the experiment. The ambient pressure is 1500 bar.

experiments. Therefore, all 18 frames have to be shown on two separate pictures. A more detailed description of all electronic devices for controlling the camera system is given in another publications [4]. More experimental and data reduction details are given in Ref. 5.

3. RESULTS

Zinc melts at 682 K; its boiling temperature at atmospheric pressure is in the vicinity of 1200 K. Since our pyrometer [6] is sensitive only above 1300 K, the measurement of surface radiation for higher static pressures with the help of our pyrometer would be very uncertain, for reasons such as unknown emissivity values of liquid zinc near its boiling point and problems with proper calibration. Surface radiation measurements were used only to check the homogeneous heating of the sample, as in this case a regular pattern of the measured radiation values is obtained. From our measurements on other liquid metals, as well as from other fast-heating pulse experiments [7], we noticed that the specific heat c_p is constant for different temperatures of the liquid phase of pure metals. Temperature was calculated from enthalpy, using Hultgen's [8] selected value for liquid zinc, $c_p = 480\ \mathrm{J \cdot kg^{-1} \cdot K^{-1}}$. Since his value of c_p in the liquid state is valid only

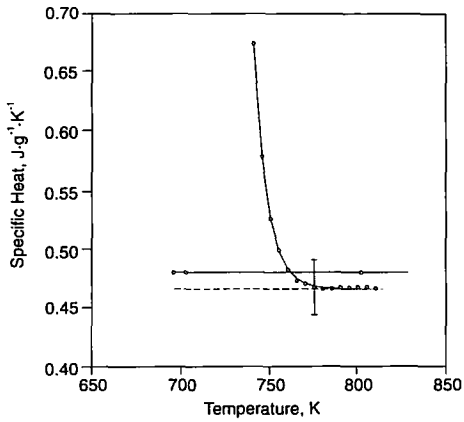

Fig. 2. Measured heat flux difference as function of temperature of zinc, using a differential scanning calorimeter at a heating rate of 20 $K \cdot s^{-1}$. The asymtotic behavior of the trace represents the heat capacity with the assumption of a constant value. Open squares are values given in Ref. 8. Measurements performed by E. Kaschnitz [9].

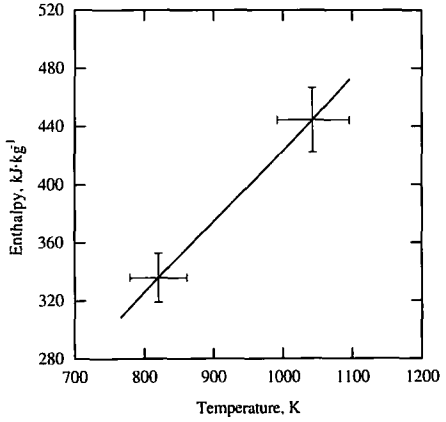

Fig. 3. Enthalpy versus temperature. Conversion of measured enthalpy values into temperature values by means of the recommended Hultgren c_p value for liquid zinc, $c_p = 480$ J · $kg^{-1} \cdot K^{-1}$.

for a small range above melting, we double-checked the specific heat capacity c_p by means of a differential scanning calorimeter in the temperature range from 400 to 800 K [9]. The results for the solid phase show excellent agreement with the recommended Hultgren values. The c_p data for the liquid phase, measured with a differential scanning calorimeter, are shown in Fig. 2. The measured values result in a c_p value of 466 $J \cdot kg^{-1} \cdot K^{-1}$ which is slightly lower than the recommended Hultgren value but still within the quoted uncertainty. Therefore, we used the Hultgren c_p value for liquid zinc, $c_p = 480\ J \cdot kg^{-1} \cdot K^{-1}$, to convert our enthalpy values into temperature values.

Figure 3 shows a plot of this conversion of our enthalpy values into temperature values with the help of the Hultgren c_p for liquid zinc. The estimated uncertainty is indicated by the error bars.

Figure 4 shows density ρ plotted versus enthalpy derived from our measurements. The least-squares fit for $300 < H < 750\ kJ \cdot kg^{-1}$ is

$$\rho = 4387.937 + 12.265H - 0.032H^2 + 1.862H^3 \tag{1}$$

where ρ is in $kg \cdot m^{-3}$.

The density ρ is plotted against temperature in Fig. 5 also, although all the information is given in Fig. 4. The least-squares fit to these data for $700 < T < 1300$ K is

$$\rho = 3315.887 + 6.448T - 0.005T^2 \tag{2}$$

where ρ is in $kg \cdot m^{-3}$.

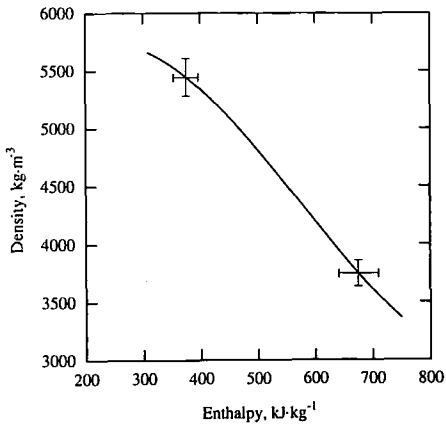

Fig. 4. Variation of density as a function of enthalpy for liquid zinc.

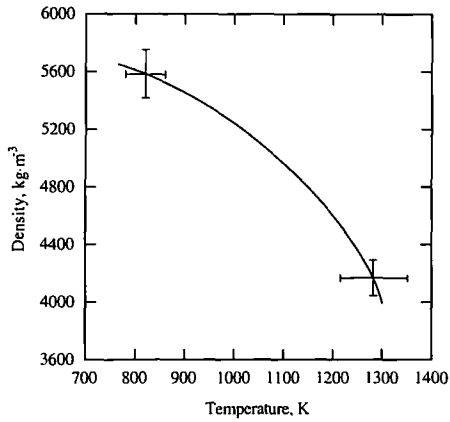

Fig. 5. Variation of density as a function temperature for liquid zinc. Conversion of measured enthalpy into temperature is made using a Hultgren c_p value for liquid zinc, $c_p = 480$ J · kg^{-1} · K^{-1}.

The measured data of volume expansion allow us to correct our data on electrical resistivity due to thermal expansion. The electrical resistivity without thermal expansion ($\Re_0$; dotted curve) and the volume-corrected values ($\Re$; solid curve) plotted against temperature are shown in Fig. 6. The least-squares fit to the data of the uncorrected electrical resistivity in the range of $700 < T < 1300$ K is given by

$$\Re_0 = -4007.582 + 21.138T + 0.044T^2 + 4.480 \times 10^{-5}T^3 - 2.279 \times 10^{-8}T^4 + 4.616 \times 10^{-12}T^5 \quad (3)$$

where $\Re_0$ is in $\mu\Omega \cdot$ m. The corrected electrical resistivity within this range is given by

$$\Re = -5.685 + 0.152T - 1.899 \times 10^{-4}T^2 + 7.442 \times 10^{-8}T^3 \quad (4)$$

For comparison, the values of Desai et al. [10] are plotted as a dashed–dotted curve; for their values, one-dimensional expansion was considered. Liquid zinc is one of the few metals with a negative slope of resistivity at the beginning of the liquid phase. At higher temperatures, the resistivity values increase again.

From our measurements, we obtain a volume-corrected value for electrical resistivity at the end of melting, $\Re = 44.5 \times 10^{-8}\ \Omega \cdot$ m, and an enthalpy at the end of melting, $H_1 = 277$ kJ · kg^{-1}.

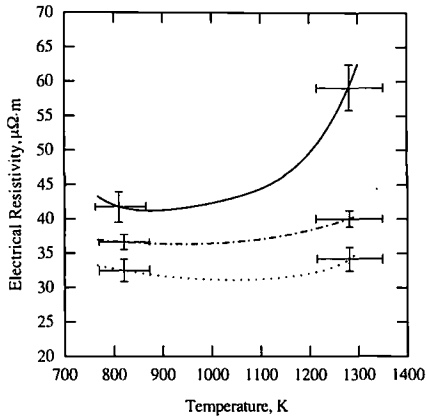

Fig. 6. Variation of electrical resistivity as a function temperature for liquid zinc. Electrical resistivity without correction for thermal expansion, dotted line; volume-corrected values, solid line; literature value, dashed-dotted line [10].

The least-squares fit to the data of the uncorrected electrical resistivity as a function of the enthalpy in the range of $300 < H < 650$ kJ · kg^{-1} is given by

$$\Re_0 = 88.648 - 0.252H + 3.362H^2 \tag{5}$$

where $\Re_0$ is in $\mu\Omega \cdot$ m. The corrected electrical resistivity within this range is given by

$$\Re = 54.171 - 0.104H + 1.174 \times 10^{-4}H^2 \tag{6}$$

As reported in Ref. 11, a strong rise in uncorrected resistivity values for higher enthalpy values has to be correlated with a strong increase in volume, if this phenomenon is described with the so called phase explosion. For our measurements on liquid zinc, increasing resistivities are always found together with increasing volumes. For other metals, when there is no volume increase, the detection of an increased resistivity could be associated with the acoustic properties, as given in Ref. 11 for liquid cerium. Reference 11 reports that the change of the acoustic characteristics might be correlated with an effect of the delocalization of the 4f electrons and thus to the change in concentration of the conducting electrons. Measured values for electrical resistivity at the end of melting compared with literature data are given in Table I.

Table I. Thermophysical Properties of Zinc: Electrical Resistivity Without Correction for Thermal Expansion at the End of Melting, $\Re_0$, Compared with the Values of Other Investigators

Investigator (first author)	Ref. No.	$\Re_0$ ($10^{-8}\,\Omega \cdot m$)
This work		34.4
Desai	10	37.46
Martynyuk	12	28.3
Martynyuk	13	38.2
Nicol'skii	14	37.5
Peletski	15	35.7
Romanova	16	29.0

4. CRITICAL-POINT DATA

Figure 7 shows a generalized phase diagram in the p–V plane. The three main areas are the region of the solid state (s), liquid state (l), and gaseous state (g). Mixtures where two states can exist at the same time are the solid–liquid region (between the s and the l region) and the liquid–vapor (l + v) and solid–vapor (s + v) regions. The line A–K is the equilibrium boiling line; A–K–D is the binodal line. The line B–K–C represents the spinodal line; K is the critical point.

The binodal line is the equilibrium curve for liquid and vapor; in the region A–K–B a mixture of liquid and vapor as well as a superheated liquid state can exist. The spinodal line B–K is the boundary of thermodynamic stability of the superheated metastabile liquid. Using high heating rates we can superheat liquid metals up to the spinodal line [17]. Close to the spinodal volume fluctuations begin (sudden growth of homogeneous vapor nuclei in the superheated liquid; see, e.g., Refs. 18 and 19. The area within B–K–C is unstable and therefore a "jump" into the region K–C–D (the so-called phase explosion) [19], where a large increase in volume will occur.

Possible changes of the state variables during our pulse heating experiment, at two static pressures, are indicated as broken lines in Fig. 7. The sample is heated from the solid state to the melting transition and through the liquid region into the region of metastabile superheated liquid. In that metastabile region, a slight increase in pressure will occur because of the volume expansion and the interaction with the surrounding water. Calculations [20] show that, at elevated pressures of 0.4 GPa, these dynamic components do not exceed 0.02 GPa for an experiment similar to ours.

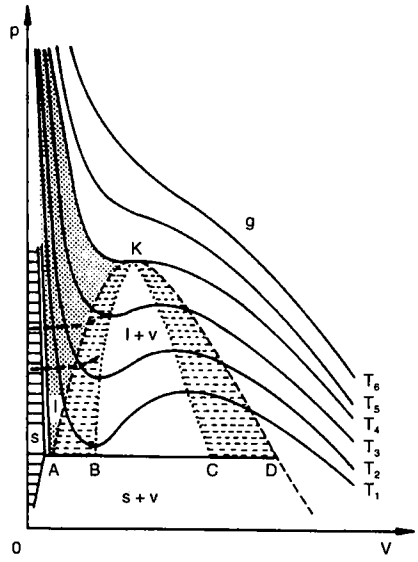

Fig. 7. Schematic van der Waals phase diagram in the p–V plane. Isotherms $T_1 < T_2 < T_3 < T_4 < T_5 < T_6$; T_4, critical isotherm; A–K–D, binodal line, B–K–C, spinodal line; K, critical point; s solid; l, liquid; v, vapor; g, gas. Broken lines indicate paths of experiments at two ambient pressures.

For the experimental determination of critical-point data, we proceeded in the following way: crossing the spinodal line causes a rapid creation of vapor nuclei connected with a powerful expansion, the phase explosion. If the static pressure p_s is increased, this phase explosion occurs at higher enthalpy values and becomes weaker. At static pressures higher than the critical pressure this phase explosion vanishes, since no drastic volume change is possible anymore. This is another approach to determine p_c in rapid resistive pulse heating experiments—simply by monitoring the sample geometry. The critical temperature T_c is estimated from the corresponding enthalpy values. The critical volume is calculated from the measured sample radius at these surroundings.

For zinc, the above-discussed pressure-dependent behavior of the phase explosion is shown in Figs. 1, 8, 9, and 10. In Fig. 1 a typical phase explosion can be seen 44.5 μs after the start of the experiment. The ambient pressure is 1500 bar. For all pressures below this value the same behavior has been noticed. In Fig. 9 at an ambient pressure of 2350 bar, the liquid phase can be maintained stable up to 50.6 μs for the same discharge

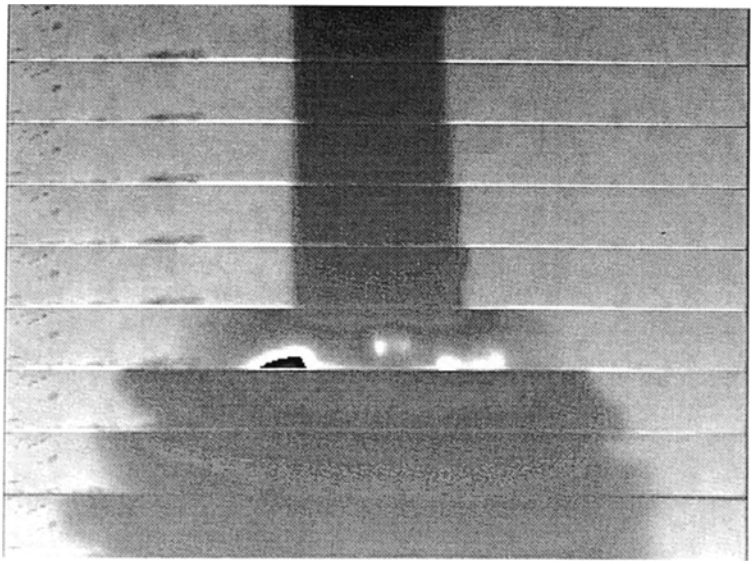

Fig. 8. Phase explosion of a zinc wire; picture taken with a fast-framing CCD-camera. The phase explosion can be seen in the sixth frame from the top, 50.6 μs after the start of the experiment. The ambient pressure is 2350 bar.

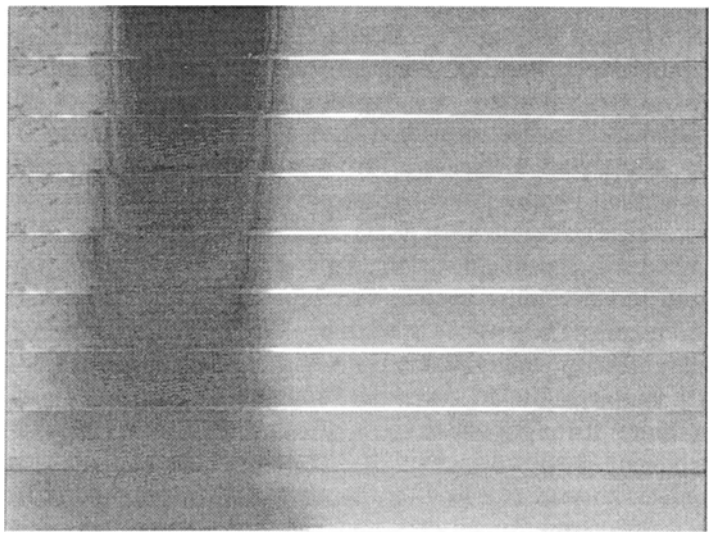

Fig. 9. Short-time frames at an ambient pressure of 3700 bar. No phase explosion can be observed. Timing between two frames, 10.13 μs.

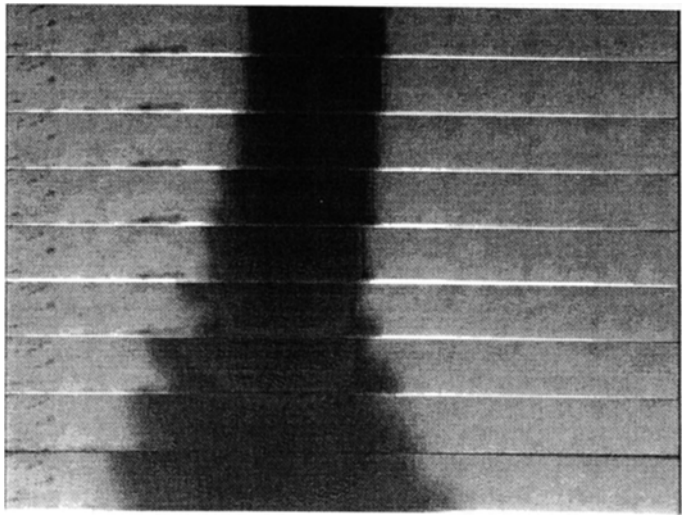

Fig. 10. Short-time frames at an ambient pressure of 3750 bar. No phase explosion can be observed. Timing between two frames, 10.13 μs.

parameters as in Fig. 1. Also the phase explosion in row 6 from the top becomes much weaker. Both effects agree with the considerations discussed above for Fig. 7. In Fig. 9 (ambient pressure, 3700 bar) and in Fig. 10 (ambient pressure 3750 bar) no phase explosion can be observed. This leads to the assumption that both experiments are performed at ambient static pressures above the critical pressure of zinc, and therefore no drastic change in density is possible above the critical pressure.

Table II. Values for the Critical Volume, V_c, the Critical Pressure, p_c, and the Critical Temperature, T_c, Compared with Literature Data

Investigators (first author)	Ref. No.	V_c ($cm^3 \cdot mol^{-1}$)	T_c (K)	p_c (bar)
This work		$25 \pm 10\%$	$3600 \pm 10\%$	$3500 \pm 5\%$
Gates	22	22.6	2169	232
Grosse	23		3380	
Kolgatin	24		3190	2630
Kopp	25		2910	
Lang	26		3390	
Martynyuk	27		3240	1740
Morris	28		2590	750
Young	29	32.6	3170	2904

More detailed investigations lead to a critical pressure value of 3500 bar. The corresponding critical volume has been found with the help of short-time pictures to be 25 $cm^3 \cdot mol^{-1}$. From the corresponding enthalpy values a critical temperature of about 3600 K was extrapolated, as explained earlier. The critical point data are compared in Table II with those of other investigators, which were all obtained by theoretical considerations.

As suggested in Ref. 30 for the critical compressibility factor z_c given by

$$z_c = \frac{p_c V_c}{R T_c} \tag{7}$$

(where p_c is the critical pressure, V_c is the critical volume, R is the molar gas constant, and T_c is the critical temperature), a value of 0.3 for z_c is obtained, which is in good agreement with experimental values for the alkali metals [39], ranging from 0.2 to 0.3.

5. ESTIMATION OF UNCERTAINTIES

Enthalpy is the most accurate quantity of all those determined under dynamic conditions. The estimated uncertainty of these values is $\pm 5\%$. The uncertainty in the uncorrected electrical resistivity is estimated to be $\pm 5\%$, increasing to $\pm 10\%$ for the corrected electrical resistivity. An error of $\pm 4\%$ is estimated for density. The static pressure in the surrounding water can be measured to within 2%. The estimated uncertainties of the critical point data are given in Table II.

6. CONCLUSIONS

Thermophysical properties of liquid zinc were investigated using a fast pulse-heating technique. Mutual relations among enthalpy, density, and electrical resistivity were obtained. Critical-point values of the pressure, temperature, and volume of zinc have been determined by monitoring the stability of liquid zinc samples with the aid of a fast CCD-framing camera.

Compared to published values, the data for T_c and p_c of this work are somewhat higher but still in good agreement. The trend to somewhat higher critical-point data, obtained by pulse-heating techniques, has been found for other metals too (e.g., Refs. 1 and 2), compared to theoretical estimated values. The reason for this discrepancy might be found in the theoretical method used. Calculations in Ref. 31 performed based on a soft-sphere model for liquid metals led to somewhat higher critical-point data

estimates than calculations performed by the same author [29] based on a hard-sphere model. Unfortunately in Ref. 31 no results for zinc were given.

This method used here cannot be applied for metals such as mercury, because in this case a metal–insulator transition occurs at high pressures before reaching the critical point, as indicated in Ref. 21. For metals with such a behavior rapid pulse-heating techniques will not be adequate to reach the critical point.

ACKNOWLEDGMENT

We thank E. Kaschnitz from the Österreichisches Gießerei-Institut, Leoben, Austria, for measurements of the heat capacity of liquid zinc using a differential scanning calorimeter.

REFERENCES

1. G. Pottlacher and H. Jäger, *Int. J. Thermophys.* **11**:719 (1990).
2. G. Pottlacher, T. Neger. and H. Jäger, *High Temp. High Press.* **23**:43 (1991).
3. R. W. Ohse and H. v. Tippelskirch, *High Temp. High Press.* **9**:367 (1977).
4. G. Nussbaumer, Diploma thesis, (Technical University Graz, 1993).
5. E. Kaschnitz, G. Pottlacher, and H. Jäger, *Int. J. Thermophys.* **13**:699 (1992).
6. W. Obendrauf, E. Kaschnitz, G. Pottlacher, and H. Jäger, *Int. J. Thermophys.* **14**:417 (1993).
7. R. S. Hixson and M. A. Winkler, *Int. J. Thermophys.* **14**:409 (1993).
8. R. Hultgren, P. D. Desai, D. T. Hawkins, M. Gleiser, K. K. Kelley, and D. D. Wagman, *Selected Values of Thermodynamic Properties of the Elements* (ASM, Metals Park, OH, 1973).
9. E. Kaschnitz, private communication 1995.
10. P. D. Desai, T. K. Chu, H. M. James, and C. Y. Ho, *J. Phys. Chem. Ref. Data* **13**:4 (1994).
11. M. Bovineau, J. B. Charbonnier, J. M. Vermeulen, and T. Thévenin, *High Temp. High Press.* **25**:311 (1993).
12. M. M. Martynyuk and I. Karimkhodzhaev, *Zh. Tekh. Fiz.* **44**:2360 (1974).
13. M. M. Martynyuk and V. I. Tsapkov, *Isz. Akad. Nauk SSSR Met.* **6**:63 (1974).
14. N. A. Nikol'skii and R. I. Pepinov, *Teploviz. Svoistva Tverd. Tel.* 87 (1971).
15. V. E. Peletskii, V. P. Druzhinin, and Y. G. Sobol, *High Temp. High Press.* **2**:167 (1970).
16. A. V. Romanova and E. A. Pavola, *Russ. Met.* **2**:41 (1974).
17. R. Gallob, Ph.D. Thesis (Technical University Graz, 1982).
18. G. R. Gathers, *Rep. Prog. Phys.* **49**:341 (1986).
19. U. Seydel and W. Fucke, *J. Phys. F Metal. Phys.* **8**:L157 (1978).
20. W. Fucke and U. Seydel, *High Temp. High Press.* **12**:419 (1980).
21. F. Hensel, M. Yao, and H. Uchtmann, *Phil. Mag. B* **52**:499 (1985).
22. D. S. Gates and G. Thodos, *Am. Inst Chem. Eng. J.* **6**:50 (1960).
23. A. V. Grosse and A. D. Kirshenbaum, *J. Inorg. Nucl. Chem.* **22**:739 (1962).
24. S. N. Kolgatin and A. V. Khachatur'yants, *High Temp.* **20**:380 (1982).
25. I. Z. Kopp, *Zh. Fiz. Khim.* **41**:1474 (1967).
26. G. Lang, *Z. Metallkunde* **68**:213 (1977).

27. M. M. Martynyuk and O. G. Panteleichuk, *Teplofiz. Vysokikh Temp.* **14**:1201 (1976).
28. E. Morris, AWRE Report No. 0-67/64 (UKAEA, London, 1964).
29. D. A. Young and B. J. Alder, *Phys. Rev. A* **3**:364 (1971).
30. J. F. Magill, and R. W. Ohse, *Handbook of Thermodynamic and Transport Properties of Alkali-Metals*, R. W. Ohse, ed. (Blackwell Scientific, Oxford, 1985), Chap 2.5.1, p. 73.
31. D. A. Young, *UCRL*-52352 (Lawrence Livermore National Laboratory, 1977).